

GEOPHYSICS :

Researching the Interior Dark Matter of the Earth from a Different View of the Core

TAIWAN UFOLOGY SOCIETY

HSIEN-JUNG HO

4th Fl., No. 6-1 lane 6, Tai-An Street,
Taipei 10054, Taiwan

<http://newidea.org.tw>

E-Mail : newidea@ufoho.no-ip.com

從地核的另一觀點探究地球內部的黑暗物質

何顯榮

摘 要

從另外一種不同的觀點，分析地球內部深處的構造、組成、密度和壓力，探究地球新模式。根據分析結果推論，地函下層和外核上層的化學成分相似，僅是固態岩石和液態岩漿的物態變化而已，兩者之間密度分布呈連續性。在外核低黏滯性的 F 過渡區，組成岩漿的各種氧化物和較活潑的金屬元素，產生氧化還原化學反應和重力分離作用。大量的氧化還原化學反應熱和被還原的重金屬沉澱於內核面時凝結成固態所釋放的凝固熱，成為從外核 F 過渡區到地殼之間一貫性大型對流囊的主要動力源。根據地球新模式，應用簡化方法計算，求得地球的質量是 5121.82×10^{24} g 和轉動慣量是 76126.841×10^{40} g·cm²，只有地球實際觀測值的 85.73% 和 94.82%。擬定一些合理的假設，引用超弦理論的新觀念解決上述二者的不足值，計算出地球內部可能有一黑暗物質的行星，存在於地球內部看不見的超三度的空間中，其半徑有 3700.375 公里。本研究的新地球模式，或可由錢德勒擺動的週期來證明。

Abstract

Examining the Earth's constitution, composition, density and pressure from a different view of the core, a new earth model has been developed. It is inferred that the solid rock and the molten rock or the magma change states interactively at the CMB. According to this model, the curve of density distribution is continuous, and chemical compositions are similar in both sides of the CMB. In the F transition zone of the outer core, some elements and oxides of magma undergo oxidation-reduction reactions and separate due to the gravity. The great amount of heat, produced from the chemical reactions and the solidifications at the ICB, causes the main power sources for the geodynamo of a great convection cell, which is the circulation flow of the magma and the solid or molten rock migrating up to the crust and down to the F zone and causes the topography of the core. Applying a simplified method to calculate the data of a suitable new earth model, the Earth's mass and moment of inertia are found to be 5121.82×10^{24} g and 76126.841×10^{40} g·cm², only 85.73 % and 94.82 % of the current data. The new conceptions of the Superstring theory are introduced to solve the problem of the insufficiencies. Finally a planet of the dark matter, a radius about 3700.375 km, has been figured out inside the Earth in the other space than ours. The new earth model may be confirmed from Chandler wobble.

Key Words: Earth model, Density jump, Convection cell, Chandler wobble, Dark matter, Solar-neutrino, Ten-dimensional theory.

I . Introduction

In the current Earth model utilized in seismological investigations, such as body-wave travel times, surface-wave dispersion and free oscillation periods for researching the chemical composition and the density distribution of the Earth, the portions of the crust and the upper mantle have been analyzed with satisfactory accuracy. Regarding the lower mantle and the core portion, however, there remain a number of questions to be answered. It has been well known that there are two convections circulating individually below the crust to the lower mantle and in the outer core. The mantle and the core are not in chemical equilibrium and the fine structure of the core-mantle boundary (CMB) is not well understood. Although some hypothesizes such as the existence of a D" transition zone in the lower mantle and iron combined with oxygen as the primary alloying constituent are suggested and a lot of advances of this research have come out, but there are also some discrepancies in the interior of the Earth [Creager & Jordan, 1986; Morelli & Dziewonski, 1987]. Furthermore, there is no conclusive evidence that the inner core is in thermodynamic equilibrium with the outer core. The main problem is a lack of phase equilibrium data for plausible core compositions at the appropriate conditions, added to the fact that seismological observations do not yet offer a decisive constraint on the difference in composition between the inner and outer core [Jeanloz, 1990].

In the early time around 1960, the composition of the outer core was devoted to the possibility that either (1) the core was a high pressure liquid phase of a magnesium or iron silicate, probably a material which was chemically consistent with the material of the bottom of the mantle, or (2) that the core was a molten form of the iron group of metallic elements [Scheidegger, 1976]. After the experiment of shockwave was performed, and the high-pressure and high-temperature experiment of diamond cell was carried out, the former lost the significance. But based on the recommendation of several geophysicists in former times and a confirmed topography of the CMB in excess of 10 km height [Morelli & Dziewonski, 1987] and according to some of the metal platinum under the frozen wastes of Siberia have come all the way from the center of the Earth [Hecht, 1995], the composition of the outer core may be considered as the material of silicates which are chemically consistent with the same material of the bottom of the mantle again, in order to solve some problems in the geophysics.

In order to investigate the outer core, a different view of the deep interior should be taken to analyze the Earth's constitution, composition, temperature and pressure, and a revolution in the chemical composition may be developed.

II . The Interior Constitution of the Earth

With regard to the Earth's interior, the constitution of the deep interior is uncertain with some difficulties. In order to conduct further investigation, the Preliminary Reference Earth Model (PREM)

[Dziewonski & Anderson, 1981] is taken as the current Earth model in this paper. At the CMB of this model, the solid portion of the lowermost mantle has a density of 5.57 g/cm^3 , which jumps to 9.90 g/cm^3 in the liquid portion of the top core, a density jump of 77.74 %. According to the physiochemical data, the average density of solid matter decreases by about 10 % when it melts into liquid state in the atmosphere; However, in the PREM the density jumps significantly at the CMB. All investigations cannot confirm the data directly. So, research about the interior constitution of the Earth is needed, especially at the CMB. There are two chief factors relating to the large density jump at the CMB:

1 . The Adams-Williamson equation:

$$d\rho/dr = -GM\rho/r^2 [V_p^2 - (4/3) V_s^2] \quad (1)$$

Bullen [1940] used equation (1) to investigate the moment of inertia of the core alone, and found it ($0.57M r^2$) to exceed that of a uniform sphere ($0.4M r^2$), so that equation 1 was rejected. Birch [1952] added a term ($-\alpha\rho\tau$) to the right of the equation in order to revise it. However, the discontinuity in density at the core boundary cannot be determined directly from the revised equation. In addition, there are two soft layers in the upper part of the mantle generally consistent with low wave velocity regions. Solomon [1972] proposed that the low wave velocity region (partial melted region) is essentially due to small amounts of liquid between granules. The density of the soft layer will not increase sharply by decreasing the velocity of seismic waves. For the same reason, wave velocity decreasing below the CMB is due to the liquid state of the outer core, a physical phenomenon of the liquid state, and may be not due to a large density jump.

2 . Deducing the certain quantities of the crust and the mantle portion from the known data of the mass and the moment of inertia of the Earth, there are the great amounts of rest values. In order to match it, the ordinary way is to set a high density distribution in the core and also a high density jump at the CMB.

It is unnecessary to consider the first factor, but the second one is considered as a matter of course within the domain of current science. If the second factor is not initially taken into consideration, a different conclusion may be drawn from some statements in the topic of the CMB as follows :

1 . Ramsey [1948] and Lyttleton [1973] have challenged the concept of an iron core, suggesting that under high temperature and pressure at the CMB the mantle silicates undergo phase changes, a solid phase changing into a liquid phase in the top core, to produce the material of high density, low melting point and electrical conductivity. Ramsey's hypothesis is still accepted by a few geophysicists for several reasons.

2 . Knopoff [1965] showed that cross a phase transition near the surface, one can predict that the bulk modulus K increases by the increasing of the density ρ ; in such a way, the ratio $K/(\rho^{7/3})$ is kept constant. From the models, the bulk modulus remains essentially unchanged across the CMB. It is difficult to account for a large density jump from about 5.57 g/cm^3 to about 9.90 g/cm^3 . On this basis, it is difficult to argue in favor of the density distribution to be smoothly continuous at the CMB and a core

of silicate composition.

3. Buchbinder [1968] studied the variation in amplitude, with distance Δ , of the reflected phase PcP. He found that the amplitude-distance curve, which displays a minimum at $\Delta = 32^\circ$, was not consistent with the computed reflection amplitudes for a solid-liquid interface if the previously accepted values of V_P and density were employed. A model proposed by Buchbinder, which is consistent with the observed amplitudes, provides no discontinuity in density between the low mantle and the core. Such a model may arise if there is considerable mixing of the core material with the lowermost mantle, and vice versa.

4. A topography of the core-mantle boundary, determined from the arrival times of reflected and transmitted waves [Morelli & Dziewonski, 1987] shows the results of an inversion indicating more than 10 km of relief with 3000~6000 km scale lengths. The depressed regions of the topography are dynamically supported by down welling of cool mantle material [Gudmundsson et al., 1986; Lay, 1989].

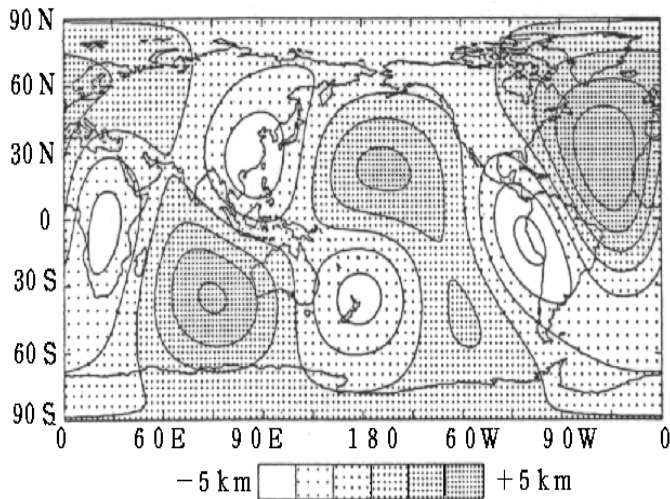


Fig 1. Topography CMB obtained by inversion of the combined PcP and PKP_{BC} Data set.

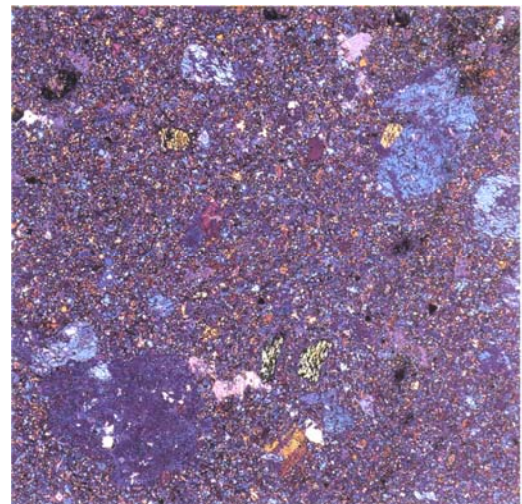


Fig 2. Hot rocks: some basalts bear platinum from the Earth's core.

5. Some of the metal platinum under the frozen wastes of Siberia may have come all the way from the center of the Earth [Jeff Hecht, 1995]. Two new studies indicate that at least some of the 2 million cubic kilometers of lava which spread over parts of Siberia 250 million years ago came from the lower mantle, up to 2900 kilometers below the Earth's surface, and a small fraction may even have come from the core itself [Walker et al., 1995; Basu et al., 1995].

In three-dimensional maps of the Earth's interior the topography of the core, different from that predicted by the hydrostatic equilibrium theory, contains information important to geodynamic processes and the geomagnetic secular variation. The topography on the CMB is likely to result from convection in the overlying mantle [Young and Lay, 1987], and some agreements of that are probably determined by processes in the core [Bloxham & Jackson, 1990]. Obviously the relief is dynamically supported and provides coupling between the mantle and the core.

The lateral temperature variations near the outer core surface are very small, amounting to only a few milli-kelvin, based on $\alpha = 5 \times 10^{-6} \text{ K}^{-1}$ (Stevenson, 1987). So, the lateral temperature variations

in the outer core can be negligible and in the lowermost mantle is so small that cannot affect the flow near the core surface. The dynamo action in the core is maintained by differential heating of the core by the mantle [Ruff & Anderson, 1980].

In regions of nearly neutral stability in the outer core an analysis of convective vigor indicates an upper bound of fractional lateral density variations of $|\delta\rho/\rho| \leq 10^{-8}$ [Stevenson, 1987]. The level of large-scale lateral heterogeneity in the outer core is below the detectable level. This is lateral homogeneity of the liquid core, so, the lateral density variations in the top of the outer core are so small that it can not provide a relief in excess of 10 km at the CMB, which may have a mechanical rather than thermal effect on the flow [Gubbins & Richards, 1986].

According to the PREM, iron is the major component of the core, and there is a density jump of 77.74 % (4.33 g/cm^3) at the CMB. Neglecting the gravity anomaly, the pressure of lateral difference at the lowermost level of the CMB is 4.246 k bar considering a relief height of 10 km. This pressure can produce an increasing iron density of $6.323 \times 10^{-3} \text{ g/cm}^3$ under conditions at there and yields a fractional lateral density variations of $\delta\rho/\rho = 0.639 \times 10^{-3}$, which is far beyond the upper bound of fractional lateral density variations of 10^{-8} . So, the density jump of 77.74 % at the CMB may be considered as an unreasonable basis of reference. Thus based on the topography, the idea of a spherical structure of the CMB in the Earth model of the PREM has been challenged, and a new study is necessary to determine the actual model.

On the basis of some of the metal platinum in Siberia may have come all the way from the center of the Earth, the idea of D" layer, which is considered to be virtually isolated the core from the rocky mantle and to sustain the chemical and the thermal equilibriums between the mantle and the core, may be challenged. It is obviously in terms of the geodynamic processes that only the vertical interactions of material and the temperature between the lowermost mantle and the outer core are the main cause. In order to maintain the 10 km of relief, the density difference between the liquid state and the solid state at the CMB must be very small or nearly equal. There is a significant suggestion that the similar materials, dominantly silicates, of the rocky mantle and the liquid outer core change states each other at the CMB to produce the core topography. A reasonable way may be figured out that the migrating masses of rock or molten rock sink downward and magma or plume rise upward in a great convection cell from the F transition zone of the outer core to the crust. A schematic diagram of the scenario is shown in Figure 3.

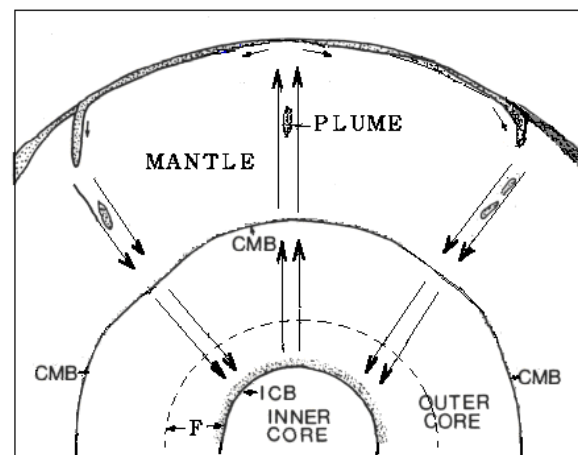


Figure 3. A schematic diagram of the great convection cell: a circulation of magma or plume and solid or molten rock migrates up to the crust and down to the F zone of the outer core and causes a topography of the core.

At the inner core boundary (ICB), a density jump of about 1.6 g/cm^3 was calculated [Bolt & Qamar, 1970]. Bolt [1972] clearly observed both low angle and steep incident reflections PKiKP of about one second period at the ICB. The mean amplitude ratio PKiKP/PcP suggests a density jump of 1.4 g/cm^3 here. Recently the density jump at the ICB has been deduced from the amplitude ratio PKiKP/PcP, and the density jump of $1.35 \sim 1.66 \text{ g/cm}^3$ there has been obtained for a quality factor in the outer core higher than 10,000 [Souriau & Souriau, 1989]. At the ICB, a density jump of 0.68 g/cm^3 in the PREM is too small to compare with the other data.

From this information other than the PREM, the density jump between the lighter liquid outer core and the solid inner core seems to be too large to represent a simple volume change on condensing as the same components change from a liquid state into a solid state. The composition of the outer core is not likely to be the same as the inner core, since a liquid in equilibrium with a solid phase in a multi-component system does not have the same composition as the solid [Hall and Murthy, 1972]. In order to confirm a favorable constitution of the Earth, the chemical composition of the core must be further investigated.

III. The Chemical Composition of the Core

The composition of the Earth's core is one of the most important and elusive problems in geophysics. There is no perfect explanation of the chemical equilibrium between the core and the mantle, and the inner core is not in thermodynamic equilibrium with the outer core.

The physical and chemical properties of the lower mantle are poorly known, and the understanding of the coupling mechanisms between the mantle and the core is poor on all timescales. But the CMB sets boundary conditions for processes occurring within the core that is a well-known fact. The topography and the lateral temperature variations in the lowermost mantle may have an indistinguishable effect on the magnetic field [Bloxham & Gubbins, 1987]. Secular variations with periods shorter than a million years, but longer than several years, almost certainly originate from processes operating in the outer core; unfortunately, there is not yet consensus as to what those processes are [Mcfadden & Merrill, 1995].

In three-dimensional maps, topographic models represent an instantaneous, low-resolution image of a convecting system. Detailed interpretation knowledge of mineral and rock properties that are, as yet, poorly known is required. A complex set of constraints on the possible modes of convection in the Earth's interior that have not yet been worked out; this will require numerical modeling of convection in three dimensions. Thus the interpretation of the geographical information from seismology in terms of geodynamical processes is a matter of considerable complexity [Woodhouse & Dziewonski, 1989]. The topography on the CMB can be sustained only by dynamic processes, and these processes must be crucially understood.

The fine structure of the CMB is not well known, but it contains information important to the geodynamic processes in the mantle or in the magnetic field generated in the outer core [Dziewonski &

Woodhouse, 1987]. Approaching the Problem of the CMB, Creager and Jordan [1986] studied travel-time anomalies of PKiKP and PKP_{AB} and corrected for the mantle structure onto a region in the vicinity of the CMB. They consider three hypotheses with regard to the source of anomalies:

the thin, heterogeneous D" region above the CMB, perturbations in the CMB topography, and a thin, highly heterogeneous layer below the CMB. Based on the great convection cell a relief of the core in excess of 10 km in provided by the three-dimensional maps may be accepted.

As stated previously, the main components of the outer core are similar to the main components of the lower mantle, i.e. silicates. Based on mineralogy, the main mineral of the mantle is pyrolite, a compound of silicates, and the main components of the outer core are also pyrolite but only in a liquid state. Under the same conditions, the higher the temperature under which common minerals are produced, the lower the polymerization is and vice versa. The closer the crystal minerals of the mantle under the temperature and pressure are to the core, the more the polymerization losses of crystalline mineral. Then the bonding forces of mineral compound are destroyed and the crystallization gradually diminishes. For example, olivine, an important rock of the Earth, under room temperature and pressure is a complex crystal tectosilicate. Quartz is a mineral of olivine. After heating, quartz, the four oxygen and four different structures of the silicon oxygen tetrahedron, are gradually reduced to tetrahedron become an elemental unit of silicates known as sorosilicates. When the temperature reaches the melting point, the sorosilicates become the nesosilicates, which are the crystal tetrahedron of silica mineral, a basic structural unit of minerals.

At the CMB under its phyllosilicates, inosilicates and cyclosilicates, respectively, when the temperature rises considerably high, the four oxygen of silicon oxygen pressure, the temperature ($4500 \pm 500^\circ \text{K}$) reaches the melting point of solid rock, and some of the rock melts in the core and liquefies into the molten rock. In the F zone of the deeper core, $5500 \sim 6600^\circ \text{K}$, polymerization may cease completely, and mostly bonding power of ions loses, only the electronic bonding force exists. All the ions and molecules may become unbounded. Therefore, the molten rock or magma becomes a mixture of oxides such as FeO, MgO, NiO, SiO₂, Fe₂O₃, Al₂O₃, Cr₂O₃, etc., and metals, such as e, Ni, Mn, etc..

In the higher resolution models, some of the heterogeneities extend upward from the CMB into the mantle in a manner suggestive of rising plume structure [Young and Lay, 1987]. Knittle and Jeanloz (1991) also suggest that a significant amount of the energy driving mantle convection is generated in the core. On this basis, a great quantity of magma heated by the extreme temperatures in the core solidifies into rock and produces the heat of solidification at the CMB. A few quantity of magma absorbing the heat does not solidify, but mixes with masses of rock as honeycombed blobs of rock rising upward at approximately an inch a year through the mantle to pour out at cracks in the mid-ocean ridge to form new ocean floor or in the continent to form great rifts. Approximately 80 % of the hot spots at the Earth's surface are manifestations of plumes rooted in the deepest part of the mantle near the CMB. The outflow

of heat is the dynamic source of continental drift. Conversely, due to convection, the downward migrating masses of cold rock in the subduction zone of the crust sink all the way through the warmer surrounding mantle to the CMB. The downward masses of rock in the cold regions of the low mantle produce depressions of the CMB into the core, and both the cold region in the mantle and a depression of the CMB produce down welling flow in the core [Bloxham & Jackson, 1990].

The energy source and buoyancy source in the core are still not well understood. But we attempt to explain this phenomenon from the perspective of the great convection cell as stated previously. The downward masses of rock absorb the heat of fusion, diminishing the heat energy at the CMB, and melting in the core where viscosity is so high that the large quantity of molten rock may not diffuse but still remain a whole. So, the components of molten rock are seldom involved in the chemical reactions.

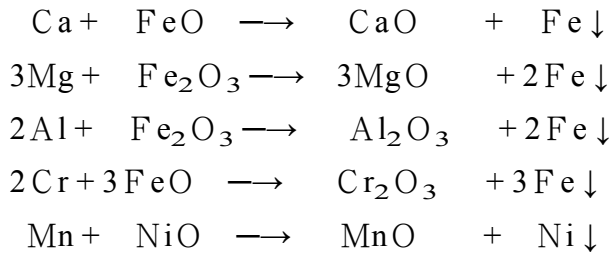
According to mechanics, although the velocity of downward migrating flow is low, the mass of the rock column from the crust to the CMB is so large that its downward momentum has a great quantity. In the liquid outer core, there is no rigid body having enough mass to counteract the downward momentum, so the molten rock sinks all the way to the inner core. The great downward momentum is counteracted by the solid inner core, which Jeanloz and Wenk [1988] have obtained a possible evidence of low-degree convection like it in the mantle in the inner core from a enigmatic observation. At the ICB, the momentum from the downward molten rock is transmitted through the core, the Earth's center and probably on to the opposite side of the CMB.

A higher resolution solution for the core velocity and wave amplitudes by A. Qamar confirms the F transition zone, 566 km in width, above the ICB [Bolt, 1972]. From ray theory, an evidence of reduced velocity gradient in a zone above the ICB has been interpreted [Rial & Cormier, 1980; Cormier, 1981], and after studying the P wave velocity recently in the F zone about 150 km above the ICB the velocity gradient is reduced to near zero [Song & Helmberger, 1995]. The P wave velocity in the F zone is nearly the same, which interprets that the magma reduces the viscosity and is able to flow more freely as the full fluid Oxides and metals, the components of magma, diffuse freely and float or sink according to its specific gravity.

There are a large amount of iron oxides (FeO , Fe_2O_3) in the mantle, and the deeper the mantle, the higher the proportion of iron oxides. An iron oxide which has metal-like density and electrical properties at high pressure and temperature exists in the Earth's core maybe a compromise between extreme views of the metallic phase and inconformity with the high cosmic abundance of oxygen [Altshuler & Sharipdzhanov, 1971]. From this information, the outer core is rich in iron oxides are proposed.

In view of the topography, the downward migrating magma rich in iron oxides is affected by diffusion, obstruction of the inner core, tangentially geostrophic flow and toroidal flow, so the fluid flows westward, which may causes the geomagnetic secular variation. Under low viscosity, the oxides and metals can vertically and horizontally flow easily, thus allowing mutual oxidation-reduction reactions to

take place in the F zone. The active light metals take oxygen from heavy metal oxides and are further oxidized into light metal oxides. The heavy metal oxides are reduced to heavy metals and sink. For example:



CaO, MgO, Al₂O₃, Cr₂O₃ and MnO float in the F zone, and Fe₂O₃, FeO and NiO become iron and nickel, which sink down to be the main component of the inner core. These oxidation-reduction reactions are exothermic processes that produce a great amount of heat. The reduced iron alloys with certain amounts of nickel and also combines with oxides to settle down at the ICB and produces the heat of solidification while it solidifies. In the F zone, magma diffuses and absorbs a great amount of heat to rise to the CMB and condenses into solid rock as the beginning of the process of large convection cell starts anew. The great amount of heat, produced from the chemical reaction in the F zone and the solidification at the ICB, causes the power sources for the geodynamo of a large convection cell. So, the Earth's geomagnetic secular variations and the geodynamical processes operate from the F zone of outer core.

As stated previously, the difference in density between the outer core and the inner core must be great. Jeanloz and Ahrens [1980] completed shock-wave experiments, in which it was found that the density of FeO is 10.14 g/cm³ when reduced to core temperature and 250 GPa pressure, and under the same conditions the density of Fe is 12.62g/cm³ [McQueen et al., 1970]. Difference between both is 2.48 g/cm³, a figure higher than all of the other evaluated values.

Figure 4 plots the PKiKP/PcP observations which contain LASA array data from Engdahl et al. [1970], Engdahl, Flinn and Masse [1974], single-station data from Buchbinder, Wright and Poupinet [1973], Warramunga array data from Souriau and Souriau [1989], and single-station GDSN data

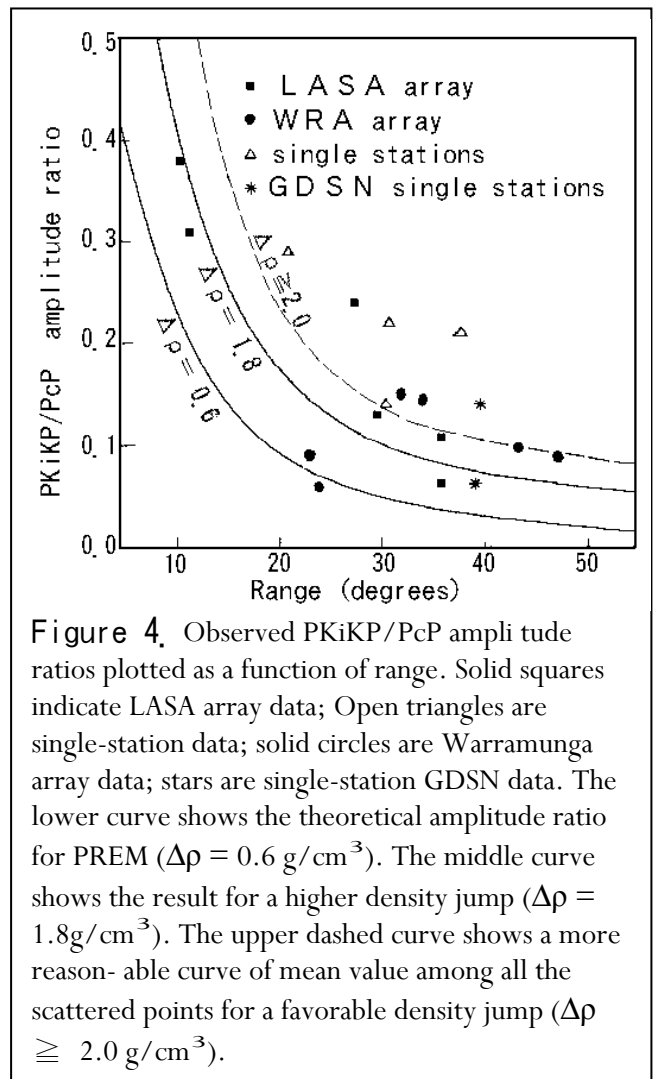


Figure 4. Observed PKiKP/PcP amplitude ratios plotted as a function of range. Solid squares indicate LASA array data; Open triangles are single-station data; solid circles are Warramunga array data; stars are single-station GDSN data. The lower curve shows the theoretical amplitude ratio for PREM ($\Delta\rho = 0.6 \text{ g/cm}^3$). The middle curve shows the result for a higher density jump ($\Delta\rho = 1.8 \text{ g/cm}^3$). The upper dashed curve shows a more reasonable curve of mean value among all the scattered points for a favorable density jump ($\Delta\rho \geq 2.0 \text{ g/cm}^3$).

from Shearer and Masters [1990]. The theoretical amplitude ratio from PREM ($\Delta\rho = 0.6 \text{ g/cm}^3$) is shown, compared with that predicted for a higher ICB density jump ($\Delta\rho = 1.8 \text{ g/cm}^3$). The data exhibit considerable scatter, but clearly favor models with higher ICB density jumps than PREM. From Figure 2, one may expect that, on average, the observed PKiKP/PcP amplitude ratio will scatter about the “true” amplitude ratio, so a dashed line ($\Delta\rho \geq 2.0 \text{ g/cm}^3$) is a more reasonable curve of mean value among all the scattered points that indicates a favorable density jump a slightly larger than 2.0 g/cm^3 .

On the basis of the free oscillation periods, Derr [1969] has inferred an Earth model DI-11 by least-squares inversion with an average shear velocity of 2.18 km/sec in the inner core and a jump in density of 2.0 g/cm^3 at its boundary, that satisfies the known mass and moment of inertia.

IV. The Evaluation of the Structure of the new earth model

In order to calculate the data of the Earth, the density distribution follows the divisions of the PREM divided into 94 levels, including 82 thin shells. The thickness of each shell is not greater than 100 km and so small compared with the Earth's radius of 6371 km, that the density is regarded as linear variation within it. Then, a simplified method is applied to calculate the information of the Earth in order to simplify the calculating work.

The mass ΔM of each shell in the Earth's interior can be calculated through

$$\Delta M = (4/3)\pi\rho_t R_t^3 - (4/3)\pi\rho_b R_b^3 \quad (2)$$

where ρ_t , ρ_b are the densities at the top and the bottom, respectively, of one shell, and R_t and R_b are the radii of the top and the bottom in a shell. Because the difference between R_t and R_b is so small and the density is regarded as linear variation in the shell, the mean value $\bar{\rho}$ of both ρ_t and ρ_b is substituted for ρ_t and ρ_b in order to simplify the calculation. Then equation (2) becomes

$$\Delta M = (4/3)\pi\bar{\rho} (R_t^3 - R_b^3) \quad (3)$$

The moment of inertia ΔI of each shell in the Earth's interior can be calculated through

$$\Delta I = (8/15)\pi (R_t^5 - R_b^5) \quad (4)$$

From fluid mechanics, in a region of uniform composition, which is in a state of hydrostatic stress, the gradient of hydrostatic pressure is expressed by

$$dp/dr = -g\rho \quad (5)$$

Where p , r are the pressure and the radius, respectively, at the region; ρ is the density at that depth; g is the acceleration due to gravity at the same depth.

If the effect of the Earth's rotation is negligible, the potential theory shows that g is resulted only from the attraction of the mass m within the sphere of radius r through

$$g = Gm/r^2 \quad (6)$$

Where G is the gravitational constant $6.6726 \times 10^{-11} \text{ m}^3/\text{kg}\cdot\text{s}^2$.

Equation (6) substitutes into equation 5 and integrate it. In order to simplify the calculation, ρ and m are substituted by $\bar{\rho}$ and \bar{m} , which are considered the constants in the thin shell and irrelative to the

ρ and r . The result becomes

$$\Delta P = (1/R_b - 1/R_t)G \bar{m}\bar{\rho} \quad (7)$$

Where ΔP is the difference in pressure between the top and the bottom in a layer of the Earth, and \bar{m} is the mass of a sphere as the mean value of the masses of the sphere within the top radius R_t and the bottom radius R_b , respectively, of a shell.

Equation (7) cannot be applied to the center of the Earth where is a discontinuous point. To integrate the portion of the center, the other form is applied as

$$\Delta P_c = (2/3)\pi G \bar{\rho}^2 R_c^2 \quad (8)$$

Where ΔP_c is the difference in pressure between the radius R_c and the center of the Earth at the center portion.

The acceleration due to gravity g of each layer can be derived from equation (6). According to the observation data, the moment of inertia about the polar axis of the Earth is $0.3309M_e R_e^2$ and about an equatorial axis is $0.3298M_e R_e^2$. The Earth is regarded as a sphere, of which the moment of inertia is determined to be 80286.4×10^{40} g.cm² by taking the mean value of both figures, where M_e is the Earth's mass of 5974.2×10^{24} g and R_e is the equatorial radius of 6378.14 km. In order to examine the accuracy of applied equations, we apply the density distribution of the PREM to calculate the Earth's mass, moment of inertia, pressure and acceleration due to gravity. The calculated values compared with that of the current data and the PREM are listed in Table 1.

Table 1. The calculated values from the density distribution of the PREM as compared with the data of the PREM and the current earth.

Data of the Earth	Mass	Moment of inertia	Pressure at CMB	Pressure At Earth center	Gravity at CMB	Gravity at Earth surface
Unit	10^{24} g	10^{40} g.cm ²	K bar	K bar	cm/sec ²	cm/sec ²
PREM & Current	5974.200	80286.400	1357.509	3638.524	1068.230	981.560
Calculated values	5973.289	80205.664	1358.335	3655.973	1068.680	981.959
Difference %	-0.0152	-0.1006	+0.0608	+0.4796	+0.0421	+0.0406

From Table 1 the deviations of the calculated Earth's values from the data of the PREM and the current Earth are nearly within 0.1%, except the pressure at the Earth center. It indicates that the calculated values are very close to the current data and the simplified method is acceptable and useful; however, the calculated pressure of 3655.973 kbar at the Earth's center is higher than the data of the PREM of 3638.524 kbar by 0.4796 %, about 8 times of deviation at the CMB. We compare all the calculated pressures of the simplified method with that of the PREM by the curve of deviation E and show the pressure P of the PREM in Figure 5.

According to the Figure 5, the curve of deviations E from the crust to the CMB is showed nearly as a straight line, indicating that the calculated pressures have the systematic errors in view of the error theory. But from the CMB to the Earth's center, the slope of curve E sharply increases above the dashed line which is the straight line extended from the CMB. It indicates that there is a considerable discrepancy

within the core. We may suppose that the structure of the core in the PREM, which greatly affects its core pressure, is something incorrect.

In order to investigate the structure of the Earth, particularly the core, four curves of density distribution are proposed to match the known conditions. From the crust to the CMB the curves of density distribution are adopted as the same of the PREM, and from the CMB to the ICB four plotted different curves are assumed. Due to a small jump of P-wave velocity at the boundary of F transition zone in the outer core, the slope of density curve is nearly as steep as the PREM. There is a discontinuity at the ICB, so that a density jump of Derr's suggestion (2.0 g/cm³) is used. In the inner core, the same slope of density curve of the PREM is used.

The four density curves of the assumed Earth model compared with the PREM are shown in Figure 6.

The mass and the moment of inertia of four new earth models can be determined, and compare with the measured data of the Earth's mass of 5974.2×10^{24} g and moment of inertia of 80286.4×10^{40} g.cm², then the differences will be found to be very large as Table 2 is shown. The differences are the insufficiencies of the mass and the moment of inertia of the four new earth models.

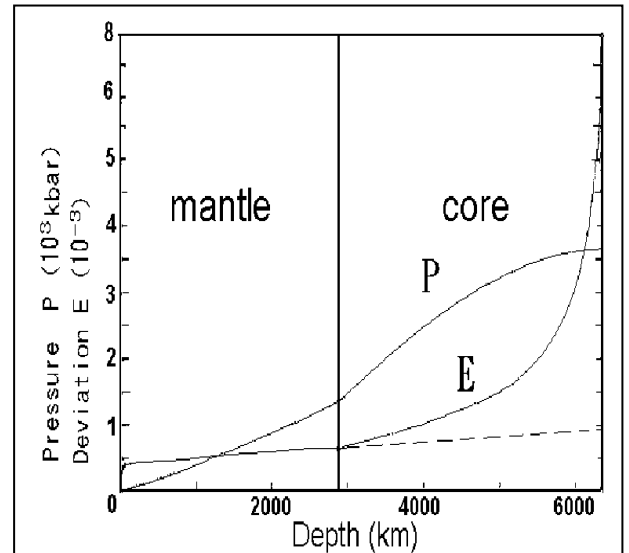


Figure 5. The pressure P of the PREM and the deviation E of the calculated pressure of simplified method from the value of P.

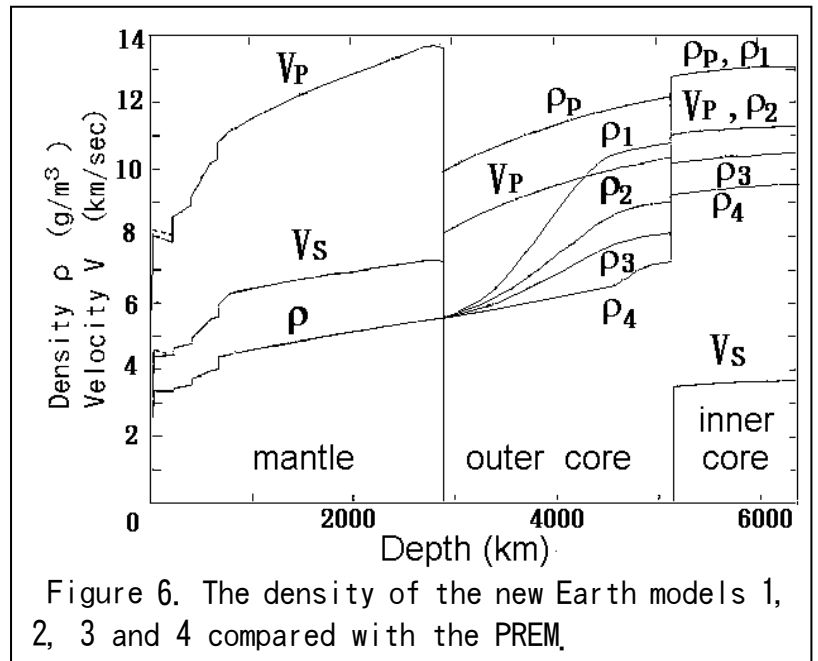


Figure 6. The density of the new Earth models 1, 2, 3 and 4 compared with the PREM.

Table 2. The insufficiencies of the mass and the moment of inertia in the four new earth models are showed.

Earth model	Unit	Observed value	New model 1	New model 2	New model 3	New model 4
Mass	10^{24} g	5974.200	5409.024	5268.126	5204.761	5121.820
Insufficiency	10^{24} g		565.176	706.074	769.439	852.380
Moment of inertia	10^{40} g.cm ²	80286.400	77007.472	76571.028	76378.768	76126.841
Insufficiency	10^{40} g.cm ²		3278.928	3715.372	3907.632	4159.559

The insufficiencies of the mass and the moment of inertia of the Earth, relative to the gravity, can only be obtained by comparing the observed data of the Earth, but it cannot be detected directly and cannot be answered clearly through the ordinary Earth sciences. If we can successfully explain that the insufficiencies exist in a suitable condition, a new earth model will be established.

The insufficiencies of the Earth's mass, called the missing mass, and moment of inertia both are relative to the gravity and belong to the dark matter in astrophysics. In this study, the insufficiencies of the mass and the moment of inertia of the Earth may belong to the dark matter in our world. In order to solve the problems of the insufficiencies, a new study of the Earth is attempted by utilizing the contemporary physics.

When stars at the outside edge of a galaxy are orbiting at high speed, the total mass of the galaxy, whose gravity keeps stars from escaping, can be estimated from the mass of the stars and its speed of rotation. Also the total mass of stars in a galaxy can be estimated by observing the galaxy with an astronomical telescope, which is less than 10 % of the estimated total mass from the orbiting stars. The phenomenon appears throughout the universe. Unobservable matter, amounted to more than 90 % mass of all the universe, is called the dark matter, which can only be detected by its gravitational influence on visible matter. Almost all astronomers agree on the existence of the dark matter; however, after more than twenty-year search, they have not found any evidence of it. Therefore, the dark matter, the densest matter in the universe, is a major problem, which still has no solution.

There are two types of the dark matter: the hot dark matter (HDM) and the cold dark matter (CDM). The HDM exists as such in a kind of photon or neutrino which has zero mass and moves at or approaching the speed of light. The CDM exists at a lower energy and particle type. Due to the gravity of the particles, the CDM moves at a low speed and collects together like normal matter. According to the observation data of background radiation in the universe, some physicists have recently proposed that perhaps the CDM explains the cosmic-structure, and the CDM model for the formation and distribution of galaxies in the universe is successful, and the expansion of the universe is dominated by the CDM [Blumenthal et al., 1984].

Proceeding with the assumption, the missing mass and moment of inertia of the Earth are those of the CDM which may constitute a normal planet. In order to find some solution in this article, the dark matter is compared to Mars. The average radius of Mars is 3397 km and the mass is 642.40×10^{24} g. Its mass approaches the insufficient mass of the new earth model 2 in the Table 3. So, the dark matter is considered as a planet, called a dark planet, of which the form is similar to Mars and its characteristics are based on the inner planets of the solar system. In order to cut a figure of the dark planet, it is considered as a sphere, whose radius and density can be calculated from the insufficiencies of the mass and the moment of inertia of the Earth through the simplified method. The data of the dark planet can be calculated as follows.

Considering the density of rock on the surface of the Earth and the moon, the surface density 2.70

g/cm^3 of the dark planet is proposed. Under the condition that the density of a layer is proportional to its depth, a trial value of density at the center of the dark planet is selected, and applying the equations (3) and (4) to calculate the mass and the moment of inertia of each shell, the total mass and moment of inertia of it should be gotten. Because the radius and the center density of the dark planet are the hypothetical values, but the total mass and moment of inertia are necessary to correspond to the insufficiencies of the Earth's; therefore, it is necessary to use a trial-and-error approach to determine the proper radius and the center density.

In order to search for the location of the dark planet in the universe, the most advanced physical theory —“Superstring theory”, is introduced to solve the problem. Superstring theory attempts a broader exploration than Einstein's Relativity theory. This theory is deduced from the characteristics of String theory and Supersymmetry and the most promising hope for truly unifying the scale of the microcosm and the macrocosm, which completes the descriptions of both in quantum field theory and General Relativity. Crudely speaking, it can unify the four basic interacting forces of nature and various elementary particles of the universe. This theory, a candidate for “theory of everything” is based on the universe constitution of nine-dimensional space and one-dimensional time and has Supersymmetry of $E_8 \otimes E_8$. However, Super-string theory, called ten-dimensional theory, is now not established as well as Relativity theory. The problem rests with the former failure, in so far as working out a theoretically solid basic geometry is highly concerned. Because there is no the exact boundary condition to fit the real universe, though many mathematicians and physicists have attempted to break the constitution of ten-dimensional space-time model down to a four-dimensional one as our known world, no proposed method meets perfection.

On October 29 in 1987, At Harvard University, the renown cosmologist — Professor A. Linde, lectured that since the universe was produced from the “Big Bang” ten-dimensional space-time of the universe is unnecessarily broken down into a four-dimensional space-time, and the other numbers of dimensional space-time may exist. Supersymmetry is one of the most elegant of all symmetries, although there is no empirical data to support the notion of highly desirable theoretical mechanisms that hold tremendous promise. But Hall [1991] reported that the physicists of CERN announced the first experimental evidence for Supersymmetry. According to Supersymmetry, every dimension of nine dimensional spaces must have the property of global symmetry with equivalent mathematical weight, so every dimension all is symmetric. The universe need not be broken down into the local symmetry when its vacuum high-energy phase transits into a low-energy one.

Without breaking the nine-dimensional space of the universe down, the ten-dimensional space-time is considered to universally exist. According to the “causality”, time cannot be divided into some different parts, so one-dimensional time is taken as a common standard in order of event in the universe. According to the “anthropic principle”, three-dimensional space and one-dimensional time are taken as one cosmos as our living world. Therefore, the nine-dimensional space can be divided into three portions,

and each portion has a common standard time, these mean there are three cosmoses in the universe. In other word, the framework of the universe, containing nine-dimensional space and one-dimensional time, will be established as a three-cosmic structure. The dark planet may be situated in a cosmos other than ours. The structure of the three-cosmic universe cannot be observed directly but may be recognized from the “missing neutrinos of the sun”.

According to Superstring theory, the $E_8 \otimes E_8$ supersymmetrical structure has characteristics in which each E_8 represents a single symmetrical group. One E_8 describes a world of general matter and the other E_8 describes a world of shadow matter. Between the both world of E_8 , there is no basic interactive forces except gravity. In other words, between any two different cosmoses in the three-cosmic universe no basic interactive forces affect each other except gravity, i.e. the shadow matter of the other worlds similar to the dark matter. So, the theoretic graviton in the field of gravity can penetrate all three cosmoses; however, photon (the light) cannot penetrate through other cosmoses. The researchers have observed the graviton in a global network, but they have not caught yet. The graviton has the physical characteristics: rest mass 0, charge 0, spin 2, light speed and carrying a very small amount of energy.

The neutrino has very high penetrability that can penetrate a 3,500 light-year thickness of lead, and has the physical characteristics: rest mass 0, charge 0, spin 1/2, light speed and carrying a very small amount of energy, but it has a little more than the graviton, so it have been captured. The neutrino is a kind of lepton and belongs to fermions, and the graviton is a gauge boson. Supersymmetry is one of the most elegant of all symmetries, which unites bosons and fermions into a single multiplet and describes both to be the same kind of particle. So, the physical characteristics of the neutrino and the graviton are similar to each other. About 2 % of the sun's energy is emitted in the form of neutrinos. In a South Dakota gold mine, an enormous tank of cleaning fluid placed deep underground has captured about a dozen solar neutrinos a month, which only about one-third the amount of it as the astrophysical theory predicts and about two-thirds of it disappears. This “solar-neutrino problem” has been a big mystery at the astro-particle frontier for the past three decades. Since the graviton can penetrate all the three cosmoses as the physical theory describes, if we compare the neutrino to the graviton, the solar neutrinos may uniformly emit into all the three cosmoses. The neutrinos reach the cosmos of our world only about one-third of their original amount and the other two-thirds of it may emit into the other two cosmoses, so the problem may be solved.

According to $E_8 \otimes E_8$ supersymmetrical structure, there are no interacting forces, including the electromagnetic force, between any two cosmoses in the three-cosmic structure except gravity, which is the characteristic of the dark matter in the universe. So, the dark planet, which is found through the gravity, may be in invisible cosmoses other than ours. Since the Earth's orbit around the sun may be affected by the gravity of the dark planet, but no abnormal effect on the Earth has been observed. An assumption is suggested that the gravity centers of the Earth and the dark planet coincide with each other at the same point. It is inferred from the phenomenon in which the same side of the moon always faces

the Earth that the Earth and the dark planet may rotate synchronously. It is hard to examine the existence of the dark planet directly; however, that can be recognized from “Chandler wobble”.

Referring to the orientation of the rotation axis of the Earth in space in addition to both precession and nutation, there is a wobble on the instantaneous axis of rotation of the Earth itself. The wobble alters the position of a point on the Earth relative to the pole of rotation. Chandler [1891] pointed out that there are two different kinds of the wobble periods. One is a period of 12 months and the other is a period of 14 months. The former, called annual wobble, is obviously affected by the seasonal climate. The latter, called Chandler wobble, has not been solved for a hundred years. Since that both the Earth and the dark planet spin synchronously around the same gravity center are postulated, but the rotation axes of both are impossible coinciding with each other. In other words, an angle between the two rotation axes produces the Chandler wobble as the precession and nutation due to the effects of the sun and the moon on non-parallel axes. Therefore, the effect of Chandler wobble may confirm the existence of the dark planet inside the Earth.

Assuming that the gravity centers of the Earth and the dark planet coincide at a single point and both rotate synchronously, the total values of mass and moment of inertia may be obtained from the sum of them. Based on mechanics, the gravity at each shell inside the Earth is affected by the mass of the Earth and the dark planet within its radius. The pressure difference $\Delta P'$ between the top and the bottom of a shell within the Earth is calculated through

$$\Delta P' = (1/R_{\mathbf{b}} - 1/R_{\mathbf{t}})G\bar{M}'\bar{\rho} \quad (9)$$

Where \bar{M}' is the mean value of the total mass of the Earth and the dark planet within the radius $R_{\mathbf{t}}$ and $R_{\mathbf{b}}$.

Equation (9) cannot be applied to the Earth's center. The average density $\bar{\rho}'$ of the central portion combined with the Earth and the dark planet within the radius $R_{\mathbf{c}}$ can be calculated through

$$\bar{\rho}' = (M_{\mathbf{c}} + M_{\mathbf{d}}) / [(4/3)\pi R_{\mathbf{c}}^3] \quad (10)$$

Where $M_{\mathbf{c}}$ and $M_{\mathbf{d}}$ are the masses of central portion in the Earth and in the dark planet, respectively.

The difference of pressure between the top and the center of the central portion in the Earth can be obtained through

$$\Delta P'_{\mathbf{c}} = (2/3)\pi G\bar{\rho}\bar{\rho}'R_{\mathbf{c}}^2 \quad (11)$$

Based on the characteristics of the inner planets of the solar system except Mercury, the bigger the radius of a planet, the higher the average density is. So, the radius and the average density of a suitable dark planet must be compatible with the characteristics of inner planet in solar system. The data of the four new earth models and each dark planet are compared with the data of the current Earth and the PREM listed in the Table 3. Both of the radiuses and the average density of the dark planet in the new earth model 4 are bigger than those of Mars; therefore, this model is found to be the more suitable one. In this suitable model the slope of density curve from a depth about 400 km of the upper mantle through

zones C, D and E to the upper boundary of F zone is nearly a straight line, which means the density increase in proportion to its depth in accord with general physical phenomenon. So, the new earth model 4 is acceptable as the proper new earth model.

The precise data of the Earth and the dark planet are calculated from the density distribution of the new earth model and listed in Tables 4, 5 and 6. The pressure P and the acceleration due to gravity g of the new earth model compared with the PREM are shown in Figure 7. We can find the pressure curve of the new earth model 4 is smoother than that of the PREM below the CMB. In the gravity curve of the new earth model 4, there are two

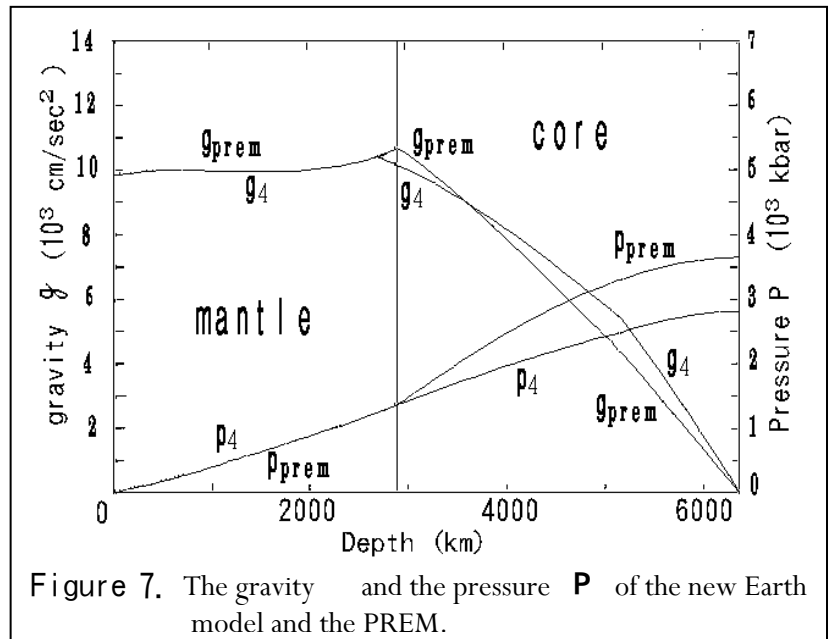


Figure 7. The gravity g and the pressure P of the new Earth model and the PREM.

deflection points in the curve that the one is at 2670.625 km in depth at the radius of the dark planet, and the other is at the ICB.

Table 3. The calculated data of the four new earth models compared with the data of the current earth and the PREM.

Kind of Earth's model	The earth planet							The dark planet					Suitability
	Radius	Ave. density	Mass of Earth	Moment of inertia	Center density	Center pressure	Moment of inertia coefficient	Radius	Ave. density	Mass	Moment of inertia	Moment of inertia coefficient	
	km	g/cm ³	10 ²⁴ g	10 ⁴⁰ g.cm	g/cm ³	kbar		km	g/cm ³	10 ²⁴ g	10 ⁴⁰ g.cm		
PREM	6371	5.5150	5974.200	80286.400	13.08848	3638.524	0.3309						
New model 1	6371	4.9935	5409.024	77007.472	13.08848	3283.754	0.3508	3808.414	2.4427	565.176	3278.928	0.4000	no
New model 2	6371	4.8635	5268.126	76571.028	11.29785	3039.584	0.3581	3732.304	3.2421	706.074	3715.372	0.3777	no
New model 3	6371	4.8050	5204.761	76378.768	10.46002	2934.587	0.3615	3717.755	3.5747	769.439	3907.632	0.3674	no
New model 4	6371	4.7284	5121.820	76126.841	9.49821	2805.297	0.3662	3700.375	4.0161	852.380	4159.559	0.3564	good

Table 4. The data of the earth planet of the new earth model are showed.

Le- vel	Radius	Density	Mass of shell	Moment of Inertia	Le- vel	Radius	Density	Mass of shell	Moment of Inertia
No.	km	g/cm ³	10 ²⁴ g	10 ⁴⁰ g.cm ²	No.	km	g/cm ³	10 ²⁴ g	10 ⁴⁰ g.cm ²
94	6371.0	1.02000			47	4000.0	5.30724	108.883	1190.942
93	6368.0	1.02000	1.560	42.192	46	3900.0	5.35706	104.551	1087.797
92	6368.0	2.60000	0.000	0.000	45	3800.0	5.40681	100.252	990.939
91	6356.0	2.60000	15.869	428.205	44	3700.0	5.45657	95.991	900.186
90	6356.0	2.90000	0.000	0.000	43	3630.0	5.49145	64.681	579.291
89	6346.6	2.90000	13.818	371.612	42	3630.0	5.49145	0.000	0.000
88	6346.6	3.38076	0.000	0.000	41	3600.0	5.50642	27.091	236.031
87	6331.0	3.37906	26.623	713.154	40	3500.0	5.55641	87.605	736.274
86	6311.0	3.37688	33.921	903.543	39	3480.0	6.56645	17.025	138.243
85	6291.0	3.37471	33.885	891.587	38	3400.0	5.60987	66.482	524.600
84	6291.0	3.37471	0.000	0.000	37	3300.0	5.66415	79.503	595.032
83	6256.0	3.37091	58.383	1531.873	36	3200.0	5.71843	75.548	532.191
82	6221.0	3.36710	57.669	1496.283	35	3100.0	5.77270	71.647	474.147
81	6186.0	3.36330	56.960	1461.353	34	3000.0	5.82698	67.805	420.694
80	6151.0	3.35950	56.254	1427.019	33	2900.0	5.88126	64.026	371.635
79	6151.0	3.43578	0.000	0.000	32	2800.0	5.93553	60.313	326.765
78	6106.0	3.46264	73.258	1834.339	31	2700.0	5.98981	56.671	285.875
77	6061.0	3.48951	72.748	1794.926	30	2600.0	6.04409	53.104	248.764
76	6016.0	3.51639	72.230	1755.876	29	2500.0	6.09837	49.616	215.223
75	5971.0	3.54325	71.702	1717.172	28	2400.0	6.15264	46.211	185.049
74	5971.0	3.72378	0.000	0.000	27	2300.0	6.20692	42.893	158.036
73	5921.0	3.78678	83.421	1966.289	26	2200.0	6.26120	39.666	133.982
72	5871.0	3.84980	83.400	1932.878	25	2100.0	6.31547	36.534	112.688
71	5821.0	3.91282	83.344	1898.957	24	2000.0	6.36975	33.502	93.955
70	5771.0	3.97584	83.256	1864.631	23	1900.0	6.42403	30.573	77.588
69	5771.0	3.97584	0.000	0.000	22	1800.0	6.47831	27.752	63.398
68	5736.0	3.98399	57.945	1278.777	21	1787.5	6.48509	3.276	7.027
67	5701.0	3.99214	57.359	1250.499	20	1700.0	6.52703	21.757	44.150
66	5701.0	4.38071	0.000	0.000	19	1600.0	6.88649	22.952	41.722
65	5650.0	4.41241	90.762	1949.III	18	1500.0	7.03784	21.027	33.736
64	5600.0	4.44316	88.027	1856.879	17	1400.0	7.09459	18.677	26.231
63	5600.0	4.44317	0.000	0.000	16	1300.0	7.15135	16.321	19.875
62	5500.0	4.50372	173.161	3556.332	15	1221.5	7.17442	11.235	11.924
61	5400.0	4.56307	169.215	3351.201	14	1221.5	9.17442	0.000	0.000
60	5300.0	4.62129	165.176	3152.302	13	1200.0	9.18575	3.636	3.554
59	5200.0	4.67844	161.058	2959.895	12	1100.0	9.23583	15.317	13.547
58	5100.0	4.73460	156.869	2774.141	11	1000.0	9.28155	12.837	9.471
57	5000.0	4.78983	152.621	2595.240	10	900.0	9.32293	10.560	6.383
56	4900.0	4.84422	148.325	2423.294	9	800.0	9.35994	8.491	4.113
55	4800.0	4.89783	143.989	2258.383	8	700.0	9.39260	6.638	2.507
54	4700.0	4.95073	139.623	2100.552	7	600.0	9.42091	5.004	1.423
53	4600.0	5.00259	135.234	1949.779	6	500.0	9.44486	3.596	0.735
52	4500.0	5.05469	130.833	1806.076	5	400.0	9.46446	2.416	0.333
51	4400.0	5.10590	126.426	1669.385	4	300.0	9.47970	1.468	0.124
50	4300.0	5.15669	122.021	1539.631	3	200.0	9.49059	0.755	0.034
49	4200.0	5.20713	117.625	1416.725	2	100.0	9.49712	0.278	0.005
48	4100.0	5.25729	113.243	1300.533	1	0.0	9.49821	0.040	0.000
Total								5,121.820	76,126.841
Insufficiency								852.380	4,159.559

Table 5. The data of the dark planet of the new earth model are showed.

Level	Radius	Density	Mass of shell	Moment of Inertia	Level	Radius	Density	Mass of shell	Moment of Inertia
No.	km	g/cm ³	10 ²⁴ g	10 ⁴⁰ g.cm ²	No.	km	g/cm ³	10 ²⁴ g	10 ⁴⁰ g.cm ²
45	3700.375	2.70000			22	1800.000	5.40184	22.932	52.388
44	3700.000	2.70053	0.174	1.590	21	1787.500	5.41961	2.7351	5.860
43	3030.000	2.80006	32.497	291.052	20	1700.000	6.64401	8.3321	37.199
42	3030.000	2.80006	0.000	0.000	19	1600.000	6.68619	9.2161	34.931
41	3600.000	2.84271	13.900	121.102	18	1500.000	6.82836	7.3881	27.897
40	3500.000	2.98488	46.148	387.849	17	1400.000	6.97063	6.6931	21.899
39	3480.000	3.01332	9.181	74.550	16	1300.000	6.11271	3.843	16.858
38	3400.000	3.12706	36.526	288.220	15	1221.500	6.22431	9.675	10.269
37	3300.000	3.26923	45.106	337.590	14	1221.500	6.22431	0.000	0.000
36	3200.000	3.41140	44.340	312.352	13	1200.000	6.25488	2.471	2.415
35	3100.000	3.55358	43.427	287.389	12	1100.000	6.39706	10.520	9.304
34	3000.000	3.69575	42.376	262.917	11	1000.000	6.53923	8.968	6.616
33	2900.000	3.83792	41.198	239.129	10	900.000	6.68140	7.604	4.536
32	2800.000	3.98010	39.904	216.189	09	800.000	6.82358	6.138	2.973
31	2700.000	4.12227	38.504	194.231	08	700.000	6.96676	4.881	1.844
30	2600.000	4.26445	37.010	173.370	07	600.000	7.10793	3.743	1.005
29	2500.000	4.40662	35.431	153.693	06	500.000	7.26010	2.736	0.559
28	2400.000	4.54879	33.780	135.269	05	400.000	7.39227	1.871	0.258
27	2300.000	4.69097	32.066	118.145	04	300.000	7.63445	1.167	0.098
26	2200.000	4.83314	30.300	102.346	03	200.000	7.67662	0.605	0.027
25	2100.000	4.97532	28.493	87.885	02	100.000	7.81880	0.227	0.004
24	2000.000	5.11749	26.655	74.754	01	0.000	7.96097	0.033	0.000
23	1900.000	5.25966	24.798	62.933					
Total								852.380	4,159.559

Table 6. The global data of the new earth model are showed.

Level	Radius	Density	Mass of shell	Mass Within Radius	Moment of Inertia	Moment within Radius	Pressure	Gravity
No.	km	g/cm ³	10 ²⁴ g	10 ²⁴ g	10 ⁴⁰ g. cm ²	10 ⁴⁰ g. cm ²	k bar	cm/s ²
94	6371.0	1.02000		5974.200		80286.400	0.000	982.108
93	6368.0	1.02000	1.560	5972.640	42.192	80244.208	0.301	982.778
92	6368.0	2.60000	0.000	5972.640	0.000	80244.208	0.301	982.778
91	6356.0	2.60000	15.869	5956.771	428.205	79816.003	3.369	983.871
90	6356.0	2.90000	0.000	5956.771	0.000	79816.003	3.369	983.871
89	6346.6	2.90000	13.818	5942.953	371.612	79444.391	6.051	984.499
88	6346.6	3.38076	0.000	5942.953	0.000	79444.391	6.051	984.499
87	6331.0	3.37906	26.623	5916.330	713.154	78731.237	11.244	984.924
86	6311.0	3.37688	33.921	5882.409	903.543	77827.694	17.900	985.494
85	6291.0	3.37471	33.685	5848.724	891.587	76936.107	24.555	986.091
84	6291.0	3.37471	0.000	5848.724	0.000	76936.107	24.555	986.091
83	6256.0	3.37091	58.383	5790.341	1531.873	75404.234	36.203	987.201
82	6221.0	3.36710	57.669	5732.672	1496.283	73907.952	47.850	988.398
81	6186.0	3.36330	56.960	5675.712	1461.353	72446.598	59.500	989.682
80	6151.0	3.35950	56.254	5619.458	1427.019	71019.579	71.151	991.056
79	6151.0	3.43578	0.000	5619.458	0.000	71019.579	71.151	991.056
78	6106.0	3.46264	73.258	5546.201	1834.339	69185.240	86.546	992.606
77	6061.0	3.48951	72.748	5473.453	1794.926	67390.314	102.086	994.187
76	6016.0	3.51639	72.230	5401.223	1755.876	65634.438	117.771	995.799
75	5971.0	3.54325	71.702	5329.521	1717.172	63917.266	133.601	997.445
74	5971.0	3.72378	0.000	5329.521	0.000	63917.266	133.601	997.445
73	5921.0	3.78678	83.421	5246.099	1966.289	61950.978	152.340	998.485
72	5871.0	3.84980	83.400	5162.699	1932.878	60018.100	171.412	999.419
71	5821.0	3.91282	83.344	5079.354	1898.957	58119.143	190.816	000.250
70	6771.0	3.97584	83.256	4996.099	1864.631	56254.512	210.551	000.977
69	5771.0	3.97584	0.000	4996.099	0.000	56254.512	210.551	000.977
68	5736.0	3.98399	57.945	4938.154	1278.777	54975.735	224.498	001.478
67	5701.0	3.99214	57.359	4880.795	1250.499	53725.236	238.480	002.036
66	5701.0	4.38071	0.000	4880.795	0.000	53725.236	238.480	002.036
65	5650.0	4.41241	90.762	4790.033	1949.111	51776.126	260.941	001.237
64	5600.0	4.44316	88.027	4702.006	1856.879	49919.246	283.099	000.466
63	5600.0	4.44317	0.000	4702.006	0.000	49919.246	283.099	000.466
62	5500.0	4.50372	173.161	4528.845	3556.332	46362.914	327.829	998.981
61	5400.0	4.56307	169.215	4359.630	3351.201	43011.713	373.094	997.602
60	5300.0	4.62129	165.176	4194.454	3152.302	39859.411	418.886	996.366
59	5200.0	4.67844	161.058	4033.396	2959.895	36899.516	465.200	995.312
58	5100.0	4.73460	156.869	3876.527	2774.141	34125.375	512.034	994.483
57	5000.0	4.78983	152.621	3723.905	2595.240	31530.135	559.390	993.925
56	4900.0	4.84422	148.325	3575.581	2423.294	29106.841	607.272	993.687
55	4800.0	4.89783	143.989	3431.592	2258.383	26848.458	655.688	993.821
64	4700.0	4.95073	130.023	3291.969	2100.552	24747.907	704.651	994.386
53	4600.0	5.00299	135.234	3156.734	1949.779	22798.128	754.177	995.445
52	4500.0	5.05469	130.833	3025.901	1806.076	20992.051	804.289	997.068
51	4400.0	5.10590	126.426	2899.475	1669.385	19322.667	855.012	999.330
50	4300.0	5.15669	122.021	2777.455	1539.631	17783.035	906.379	002.317
49	4200.0	5.20713	117.625	2659.830	1416.725	16366.310	958.429	006.122
48	4100.0	5.25729	113.243	2546.587	1300.533	15065.777	1011.207	010.848

Level	Radius	Density	Mass of shell	Mass Within Radius	Moment of Inertia	Moment within Radius	Pressure	Gravity
No.	km	g/cm ³	10 ²⁴ g	10 ²⁴ g	10 ⁴⁰ g. cm ²	10 ⁴⁰ g. cm ²	k bar	cm/sec ²
47	4000.0	5.30724	108.883	2437.704	1190.942	13874.835	1064.767	1016.614
46	3900.0	5.35706	104.551	2333.152	1087.797	12787.039	1119.172	1023.550
45	3800.0	5.40681	100.252	2232.900	990.939	11796.100	1174.494	1031.804
44	3700.0	5.45657	96.165	2136.734	901.775	10894.325	1230.814	1041.459
43	3630.0	5.49145	97.178	2039.557	870.342	10023.983	1270.565	1032.803
42	3630.0	5.49145	0.000	2039.557	0.000	10023.983	1270.565	1032.803
41	3600.0	5.50642	40.991	1998.565	357.133	9666.850	1287.573	1028.983
40	3500.0	5.55641	133.753	1864.812	1124.123	8542.727	1344.157	1015.767
39	3480.0	5.56645	26.206	1838.606	212.793	8329.934	1355.440	1013.037
38	3400.0	5.60987	103.008	1735.599	812.820	7517.114	1400.496	1001.813
37	3300.0	5.66415	124.609	1610.990	932.622	6584.492	1456.591	987.097
36	3200.0	5.71843	119.888	1491.103	844.543	5739.949	1512.369	971.634
35	3100.0	5.77270	115.074	1376.028	761.536	4978.413	1567.772	955.430
34	3000.0	5.82698	110.181	1265.847	683.611	4294.802	1622.740	938.499
33	2900.0	5.88126	105.224	1160.623	610.764	3684.038	1677.213	920.853
32	2800.0	5.93553	100.217	1060.406	542.954	3141.084	1731.131	902.508
31	2700.0	5.98981	95.175	965.230	480.106	2660.978	1784.433	883.483
30	2600.0	6.04409	90.114	875.116	422.134	2238.844	1837.060	863.802
29	2500.0	6.09837	85.047	790.069	368.916	1869.928	1888.951	843.490
28	2400.0	6.15264	79.991	710.079	320.318	1549.610	1940.047	822.582
27	2300.0	6.20692	74.959	635.120	276.181	1273.429	1990.291	801.116
26	2200.0	6.26120	69.966	565.154	236.328	1037.100	2039.628	779.142
25	2100.0	6.31547	65.027	500.126	200.573	836.527	2088.003	756.721
24	2000.0	6.36975	60.157	439.969	168.709	667.819	2135.368	733.934
23	1900.0	6.42403	55.371	384.598	140.521	527.298	2181.678	710.878
22	1800.0	6.47831	50.684	333.914	115.786	411.511	2226.896	687.677
21	1787.5	6.48509	6.011	327.903	12.893	398.618	2232.456	684.776
20	1700.0	6.52703	40.089	287.814	81.349	317.269	2270.939	664.522
19	1600.0	6.88649	42.168	245.646	76.653	240.617	2314.824	640.272
18	1500.0	7.03784	38.415	207.231	61.633	178.984	2358.655	614.564
17	1400.0	7.09459	34.270	172.961	48.130	130.854	2401.336	588.826
16	1300.0	7.15135	30.164	142.798	36.733	94.121	2442.566	563.807
15	1221.5	7.17442	20.910	121.888	22.193	71.928	2473.835	545.091
14	1221.5	9.17442	0.000	121.888	0.000	71.928	2473.835	545.091
13	1200.0	9.18575	6.107	115.781	5.969	65.959	2484.512	536.500
12	1100.0	9.23583	25.837	89.944	22.851	43.108	2532.405	496.000
11	1000.0	9.28155	21.805	68.139	16.087	27.021	2576.798	454.664
10	900.0	9.32293	18.064	50.076	10.919	16.102	2617.562	412.515
9	800.0	9.35994	14.629	35.447	7.086	9.016	2654.582	369.568
8	700.0	9.39260	11.519	23.928	4.351	4.665	2687.749	325.841
7	600.0	9.42091	8.747	15.181	2.488	2.176	2716.972	281.380
6	500.0	9.44486	6.332	8.850	1.294	0.882	2742.182	236.210
5	400.0	9.46446	4.287	4.563	0.591	0.291	2763.336	190.294
4	300.0	9.47970	2.625	1.938	0.222	0.069	2780.457	143.683
3	200.0	9.49059	1.360	0.578	0.061	0.009	2793.727	96.419
2	100.0	9.49712	0.505	0.073	0.009	0.000	2804.037	48.710
1	0.0	9.49821	0.073	0.000	0.000	0.000	2805.297	0.000

The Earth has a mass of 5121.820×10^{24} g, a moment of inertia of 76126.841×10^{40} g.cm², an average density of 4.7284 g/cm³, a density of 9.49821 g/cm³ and the pressure of 2805.297 kbar at Earth's center. The reduced values of the Earth's data from those of the current Earth are due to the existence of the dark planet. The dark planet has a radius of 3700.375 km, a moment of inertia of 4159.559×10^{40} g.cm², an average density of 4.0161 g/cm³ and a mass of 852.380×10^{24} g about 1.33 times of Mars. The data of the new earth model compared with those of the current Earth and the PREM are listed in Table 7.

Table 7. The data of the new earth model compared with the data of the current Earth and the PREM.

Data of planet	Radius	Mass	Inertia of moment	Average density	Center density	Center pressure	Coefficient
Unit	km	10^{24} g	10^{40} g.cm ²	g/cm ³	g/cm ³	k bar	
PREM and current earth	6371.000	5974.200	80286.400	5.515	13.08848	3638.524	0.3309
Earth planet	6371.000	5121.820	76126.841	4.7284	9.49821	2805.297	0.3662
Dark planet	3700.375	852.380	4159.559	4.0161	7.96097	1115.272	0.3564

The density of the Earth's center is 9.49821 g/cm³, which is much lower than 13.08848 g/cm³ of the PREM. Its pressure is 2805.297 kbar, which is also much lower than 3638.524 kbar of the PREM. The composition of the inner core is generally believed to be dominantly iron with a small amount of alloyed nickel. From the pressure- density Hugoniot data, the density of iron under 2805.297 kbar of pressure is about 12.7 g/cm³ [Ahrens, 1980], which is much greater than that of the new earth model 4 by 25 %. The inner core is not pure iron but contains a significant fraction of light components [Ringwood, 1984; Jephcoat & Olson, 1987], and that explains why the density of the inner core is so much smaller than the current value. So, an inference that the composition of the inner core is dominantly iron, alloyed with a small amount of nickel and also combined with a significant amount of oxides is suggested.

V. Discussion

In this discussion, the contemporary physics is introduced and a lot of assumptions are suggested in order to solve the problems of insufficiencies of the Earth's mass and moment of inertia and explore a new frontier of science.

Superstring theory has the positive figures of its fabulously large set of symmetries and miraculous

cancellations of all the potential anomalies and divergences in quantum field theory. It provides a unifying description of elementary particles and forces of nature. But it has been pointed out by critics that the model has shortcomings and potential theoretical problems [Kaku, 1988]. Among those problems, the most fundamental one is that geometric formulation of the model has not been well understood yet. If the geometry underlying the Superstring theory has been determine, that may give us the key insight into the model and will allow us to make definite predictions with the theory. After studying the existence of the dark planet in the Earth's interior, the three-cosmic structure of the universe may be able to be confirmed. If the mathematicians and physicists take the geometric framework of ten-dimensional space-time in a three-cosmic structure of the universe as a new way to explore the Superstring theory, they maybe complete it successfully in a short period of time.

From this study, the hypothesis of the three-cosmic structure of the universe maybe enable a new way to find out about the abundant dark matter and solve some problems in astrophysics such as:

1. Cygnus X-1 is a hot super giant star orbited by an invisible compact object in a period of 5.6 days [Stokes & Michalsky, 1979]. The mass of the compact object can be estimated from the Doppler shifts in the spectrum of the visible super giant star. Its mass is about 9 times of the sun. This is considerably more than the maximum mass of a neutron star. Therefore, the compact object is not a neutron star or a white dwarf star. Since it has problems of optical confirmation, it is believed that the compact object may not be a black hole (Nowadays it is considered a black hole candidate, but that is not conclusive). If we consider the compact object of Cygnus X-1 as the dark matter in the other cosmos and its gravity affects Cygnus X-1, the problem may be solved.

2. Bray [1972] deduced from the observed data that when Halley's Comet reaches the sun, the real day always precedes or lags behind the predicted day for four days. Using a computer to treat the data of it in a numerical model of the solar system, he found a tenth planet X which was about three times the size of Saturn. Flandern [1981] proposed a search for a planet X, which has about three times the mass of the Earth and a highly inclined eccentric orbit, that accounted for all of the perturbations on the motions of Neptune. In 1987, John Anderson, the American astronomer, presented the deviation of Neptune and Uranus in the regular orbit and proposed "The Theory of X Planet" from observed astronomical data of the nineteen century. The mass of X planet is about five times that of the Earth and its period is about 700 ~ 1000 years. The orbit is elliptical and the inclination from the orbit to ecliptics very large and almost perpendicular. Now the planet X has been searched for, but it still remains to be found. If the dark planet X orbits around the sun in another cosmos, then its gravity will sometimes affect the motion of Halley's Comet, Neptune and Uranus. Therefore, the problem of the invisible planet X may be solved.

3. According to the data from the telescopes of electromagnetic wave, there are 761 sources of γ ray burst nearly all over the universe. But at the direction of each γ ray burst, the telescope does not find any object of star. The γ ray burst which has very high energy (more than 100,000 EV) may penetrate into any

spaces of the three-cosmic universe, so the sources of γ ray burst may be emitted from the dark matter in the other spaces than ours.

4. The Unidentified Flying Objects (U F O) sometimes appear on the Earth, but we cannot propose an acceptable reliable theory of the U F O in the field of science which confirms their existence. If we separated the limit of the known science of cosmos to consider the three-cosmic structure of the universe, the mass of the dark matter is about ten times of our cosmos. Some dark planets may be in the other cosmoses near or within the solar system such as the tenth planet X. The Extraterrestrials (E. T.) maybe live on some of these planets. Sometimes they can fly the U F O to penetration to our space and arrive on the Earth and even land on the dark planet inside the Earth as a base. If we explain the E. T. And the U F O in this way, the problem may be solved.

V I . Conclusion

This is absolutely a new try to break the bottleneck of the research in the deep interior of the Earth and in the astrophysics, and there is no relative paper providing the reference across the two different frontiers.

Based on the new try, a study in a different view of the core, we infer that a great convection cell, a circulation of magma and solid or molten rock migrating up to the crust and down to the F zone of the outer core, causes the topography of the core and the metal platinum have come all the way from the center of the Earth. This study introduces a new earth model which should solve some inexplicable problems of the Earth, such as the density jump at the CMB, the core-mantle chemical equilibrium, the thermodynamic equilibrium of the inner and outer core, the geomagnetic secular variation and the Chandler wobble. The anomalous properties of the CMB and the ICB should be apparently brightened after this study.

From the simplified method of calculating the data of the Earth, the mass and the radius of the dark planet can be mathematically determined, and this result may be served as an indirect proof of the existence of the dark matter, which locates in other space than ours. Comparing with the observed data of the Earth, there are 14.27 % of the mass and 5.18 % of the moment of inertia missing. From the conceptions of the dark matter and the Superstring theory, a dark planet inside the Earth, whose mass and moment of inertia supply the missing portions of the Earth, is virtuously developed. The new earth model may be confirmed from the period of Chandler wobble.

From the applications of the ten-dimensional space-time and the Supersymmetry of Superstring theory, the three-cosmic structure of the universe is inferred. Some scientific problems other than the geophysics may be roughly solved, such as the dark matter, the missing solar-neutrino, the solar planet-X, the sources of γ ray burst, the U F O and the basic geometry of Superstring theory, but that still needs to be proved by the outcomes of the physicists' research. To demonstrate the three-cosmic structure of the

universe from the missing neutrinos, we can plan a project of investigating the quantity of anti-neutrino, which is emitted from nuclear plants.

Acknowledgements

I am grateful to Dr. Lin-Gun Liu of Research School of Earth Science in Australian, and Dr. Hsueh-Wen Yeh of Hawaii Institute of Geophysics for constructive criticisms and helpful comments.

References

- Altshuler, L. V. and Sharipdzhanov, L. V., 1971: On the distribution of iron in the Earth and the chemical distribution of the latter. *Bull. Acad. Sci. USSR, Geophys. Ser.*, 4, 3-16.
- Ahrens, T. J., 1980: Dynamic Compression of Earth Materials, *Science* 207, 1035.
- Basu A. R., Poreda R. J., Renne P. R., Teichmann F., Vasiliev Y. R., Sobolev N. V. and Turrin B. D., 1995: High- He plume origin and temporal-spatial evolution of the Siberian flood basalts, *Science*, vol. 269, 822-825.
- Birch, F., 1952: Elasticity and constitution of the Earth's interior, *J. Geophys. Res.*, 57, 227.
- Bloxxham, J. and D. Gubbins, 1987: Thermal core-mantle interactions, *Nature*, 325, 511-513.
- Bloxxham, J. and Jackson, A., 1990: Lateral temperature variations at the core-mantle boundary deduced from the magnetic field, *Physical Review Letters*, Vol. 17, No. 11, 1997-2000 pp.
- Blumenthal, G. R., Faber, S. M., Primack, J. R. and Rees, M. J., 1984: Formation of galaxies and large-scale structure with cold dark matter. *Nature*, Vol. 311, 517-525.
- Bolt, B. A., 1972: The Chemistry of the Earth's Core from Seismological Evidence, *May, EOS.*, Vol. 53, No. 5, 599 pp.
- Bolt, B. A., and Qamar, A., 1970: Upper bound to the density jump at the boundary of the Earth's inner core, *Nature*, 228, 148-150.
- Brady, J. L., 1972: *The Journal of the Astronomical Society of the Pacific*.
- Buchbinder, Geotz G. R., 1968: Properties of the Core-Mantle Boundary and Observations of PcP, *J. Geophys. Res.*, 73, 5901.
- Buchbinder, G. G., Wright C. and Poupinet G., 1973: Observations of PKiKP at distances less than 110 , *Bull. Seism. Soc. Am.*, 63, 1699-1707.
- Bullen, K. E., 1940: The problem of the Earth's density variation, *Bull. Seism. Soc. Am.*, 30, 235-250.
- Chandler, S., 1891: On the variation of latitude, *Astronomical Journal*, 11, 83.
- Cormier, V. F., 1981: Short-period PKP phases and the inelastic mechanism of the inner core, *Phys. Earth Plant. Inter.* 24, 291-301.
- Creager, K. C., and Jordan, T. H., 1986: Aspherical structure of the core-mantle boundary from PKP travel time, *Geophysics. Res. Lett.*, 13, 1497-1500.

- Derr, J. S., 1969: Internal Structure of the Earth Inferred from Free Oscillations, *J. Geophys. Res.*, 74, 5202.
- Dziewonski, A. M. and Anderson, D. L., 1981: Preliminary Reference Earth Model, *Phys. Earth Planet. Inter.*, 25, 297.
- Dziewonski, A. M. and Woodhouse, J. H., 1987: Global Images of the Earth's Interior, *Science*, Vol. 236, 37-48.
- Engdahl, E. R., Flinn, E. A. and Romney, C. F., 1970: Seismic waves reflected from the Earth's inner core, *Nature*, 228, 852-853.
- Engdahl, E. R., Flinn, E. A. and Masse, P., 1974: Differential PKiKP travel times and the radius of the inner core, *Geophys. J. R. astr. Soc.*, 39, 457-463.
- Flandern, T. V., 1981: The renewal of the Trans-Neptunian planet search, *Bulletin of the American Astronomical Society* 12, 830.
- Gubbins, D. and Richards, M. A., 1986: Coupling of the core dynamo and mantle: Thermal or Topography? *Physical Review Letters*, 13, 1521-1524.
- Gundmundsson, O., Clayton, R. W. and Anderson, D. L., 1986: CMB topography inferred from ISC PcP travel times, *Eos, Trans. AGU*, 67, 1100.
- Hall, N., 1991: May the forces are unified with Supersymmetry, *New Scientist*, 6 April, 11 pp.
- Hall, T. H. and Murthy, V. R., 1972: Comments on the Chemical Structure of a Fe-Ni-S Core of the Earth, *EOS.*, Vol. 53, No.5, 602 pp.
- Hecht, J., 1995: Buried treasure from hot heart of the Earth, *New Scientist*, 19 August, 16 pp.
- Jeanloz, R., 1990: The nature of the Earth's core, *Annu. Rev. Earth Planet. Sci.*, 18, 357-386.
- Jeanloz, R. and Ahrens, T. J., 1980: Equations of FeO and CaO, *Geophys. J. R. Astr. Soc*, 62, 505-528.
- Jeanloz, R. and Wenk, H. R., 1988: Convection and anisotropy of the inner core, *Geophys. Res. Lett.* 15, 72-75.
- Jeff Hecht, 1995: Buried treasure from hot heart of the Earth, *New Scientist*, 19, Aug., 16 pp,
- Jephcoat, A. and Olson, P., 1987: Is the Inner Core of the Earth Pure Iron? *Nature*, Vol. 325, 332-335.
- Kaku, M., 1988: *Introduction to Superstrings*, Springer Verlag New York Inc., New York, USA. 16-18 pp.
- Knittle, E. and Jeanloz, R., 1991: The high-pressure phase diagram of Fe_{0.94}O : A possible constituent of the Earth's core, *J. Geophys. Res.*, Vol. 96, 16, 169-180.
- Knopoff, F., 1965: *Phys. Rev.*, 138, A 1445.
- Lay, T., 1989. Structure of the Core-Mantle Transition Zone: A Chemical and Thermal Boundary Layer, *Eos*, Vol. 70, No. 4, Jan. 24, p.49, 54-55, 58-59.
- Lyttleton, R. A., 1973: The end of the iron-core age, *Moon*, 7, 422-439. McFadden, Phillip L. and Merrill

- Ronald T., 1995: History of Earth's magnetic field and possible connections to core-mantle boundary processes. *J. Geophysics. Res.*, 100, 307-316.
- McQueen, R. G., Marsh, S. P., Taylor, J. W., Fritz, J. N. and Carter, W. J., 1970: The equation of state of solids from shock wave studies, in high velocity impact phenomena, Kinslow, R., Academic Press, New York, 294-419 pp.
- Morelli, A. and Dziewonski, M., 1987: Topography of the core-mantle boundary and lateral homogeneity of the liquid core, *Nature*, Vol., 325, 19, Feb., 678-683.
- Ramsey, W. H., 1948: On the constitution of the terrestrial planets, *Mon. Not. Roy. Astron. Soc.*, 108, 406-413.
- Rial, J. A. and Cormier, V. F., 1980: Seismic waves at the Epicenter's antipodes, *J. Geophysics. Res.*, 91, 10203-10228.
- Ringwood, A. E., 1984: The Earth's Core: its composition, formation and bearing upon the origin of the Earth, *Proc. R. Soc. A*, 395, 1-46.
- Ruff, L. and Anderson, D. L., 1980, Core formation, evolution, and convection: A geophysical model, *Phys. Earth Planet. Inter.*, 21, 81-201.
- Scheidegger, Adrian E. 1976: *Foundation of Geophysics*. 294 pp.
- Shearer, P. Masters, G., 1990: The density and shear velocity contrast at the inner core boundary, *Geophysics. J. Int.*, 102, 491-498.
- Solomon, S. C., 1972: Seismic-wave attenuation and partial melting in the upper mantle of North America. *J. Geophysics. Res.* 77, 1483-1502.
- Song, X. and Helmberger, Don V., 1995: A P wave velocity model of earth's core, *J. Geophysics., Res.*, Vol., 100, No. B7, 9817-9830.
- Souriau, A. and Souriau, M., 1989: Ellipticity and density at the inner core boundary from subcritical PKiKP and PcP data, *Geophysics. J. Int.*, 98, 39-54.
- Stevenson, D. J., 1987: Limits on lateral density and velocity variations in the Earth's outer core, *Geophysics. J. R. Astr. Soc.*, 88, 311-319.
- Stokes, G. M. and Michalsky, J. J. 1979: Cygnus X-1, Mercury 8, 60. Walker R. J., Morgan J. W. and Horan M. F., 1995: Osmium-187 in some plumes: Evidence for core-mantle interaction? *Science*, Vol. 269, 819-822.
- Woodhouse, J. H. and Dziewonski, A. M., 1989: Seismic modeling of the Earth's large-scale three-dimensional structure, *Phil. Trans. R. Soc. Lond. A* 328, 291-308.
- Young, C. J. and Lay, T., 1987: The core-mantle boundary, *Ann. Rev. Earth Planet. Sci.*, 15: 25-46.